

TROMBONE SOUND SIMULATION UNDER VARYING UPSTREAM COUPLING CONDITIONS

Vincent Fréour and Gary P. Scavone

Computational Acoustic Modeling Laboratory (CAML)

Centre for Interdisciplinary Research in Music Media and Technology (CIRMMT)

McGill University

vincent.freour@mail.mcgill.ca

ABSTRACT

The acoustical influence of the upstream airways is an important issue in brass performance. Analyzing the modalities of upstream resonance adjustments around the playing frequency will improve our understanding of vocal-tract tuning and lip-valve mechanics in brass instrument playing. In this study, different conditions of upstream coupling are simulated at the fundamental frequency using a simple one-mass model of the lips coupled to a trombone resonator. Maintaining a constant amplitude of the upstream acoustic pressure, variations of the phase of the upstream relative to the downstream input impedance at the fundamental frequency f_0 result in changes in playing frequency, as well as in the downstream acoustic energy produced. Further analysis shows that this upstream acoustic control can displace the playing frequency near the lip natural frequency, allowing optimal efficiency of the mechanical lip-valve system. These results highlight the possible importance of upstream phase tuning as part of a vocal-tract tuning strategy in brass performance. It further suggests a new experimental method for the estimation of lip natural frequencies on artificial player systems.

1. INTRODUCTION

Recent measurements of vocal-tract influence in trombone and trumpet performance have highlighted the ability of proficient players to create an upstream resonance around the playing frequency that supports or even overrides the regenerative effect of the downstream air-column in the higher register [1–3]. This important contribution of upstream airways also appears to be dependent on the phase of the vocal-tract input impedance at the playing frequency. Experimental investigations conducted on an artificial player system allowed the phase of an upstream resonance at f_0 to be varied independently from the amplitude, leading to variations of the playing frequency around a downstream impedance peak, as well as changes in the downstream acoustic energy produced [4]. These results suggest that an optimal upstream phase tuning, matching with mechanical constrains from the vibrating lips, induces maxi-

mal lip displacement. In this paper, we present the results from numerical simulations using a simple vibrating lip model coupled to a downstream trombone air-column, and involving controlled upstream coupling conditions. Fritz proposed a frequency-domain simulation, as well as an analytical formulation of the frequency shift induced by a vocal-tract resonance in a clarinet model [5]. Contrary to the latter technique, the method proposed in this paper is based on the time-domain resolution of the coupled equations governing the dynamics of the system. This approach allows for the theoretical investigation of the effect of upstream phase tuning on the behaviour of this simple lip model.

2. LIP MODEL

2.1 Mechanical equation

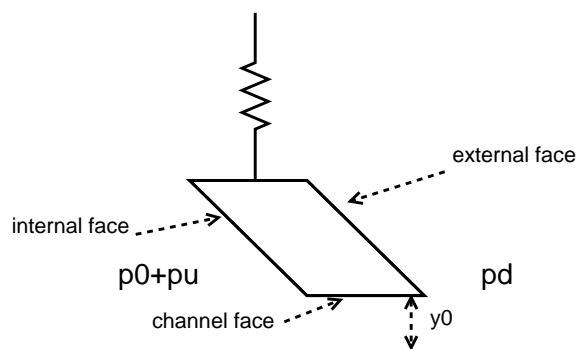


Figure 1. One-mass model of the lips.

The mechanical model chosen for the lips is inspired from [6] and presented in Fig. 1. The two lips are assumed to be identical and placed symmetrically on the mouthpiece. Each lip is allowed to move along a vertical axis and its vertical position relative to the equilibrium position y_0 is noted y . Neglecting the Bernoulli pressure applied on the channel face, an overpressure on the upstream side tends to increase the lip opening area, while an overpressure on the downstream side tends to close it. According to Helmholtz [7], this model corresponds to an outward striking model of the lips. Although a brass player's lips do not seem to support the outward striking model over the full range [8–11], we will assume, in order to keep the

problem simple, that this model adequately simulates the mechanical behaviour of a trombone player's lips over the traditional playing range. The upstream acoustic pressure (mouth side) arising from the upstream acoustical feedback is noted p_u and the quasi-static mouth pressure p_0 . The downstream acoustic pressure (mouthpiece side) arising from the downstream acoustical feedback is noted p_d . In this model, the dynamics of each lip can be represented by the simple second order oscillator equation:

$$\frac{d^2y}{dt^2} + \frac{\omega_{lip}}{Q_{lip}} \frac{dy}{dt} + \omega_{lip}^2(y - y_0) = \frac{F}{m_{lip}}, \quad (1)$$

where ω_{lip} is the lip angular frequency ($\omega_{lip} = 2\pi f_{lip}$), Q_{lip} the quality factor, m_{lip} the mass of one lip and y_0 the lip vertical equilibrium position. F is the vertical component of the force acting on the lip. F is proportional to the pressure difference between mouth and mouthpiece i.e. $F/m_{lip} = (p_0 + p_u - p_d)/\mu$, where μ is the effective mass of the lips, m_{lip} , divided by the effective area of the internal face of the lips; this force therefore supports an outward striking reed behaviour. By substituting F/m_{lip} , Eq. 1 becomes:

$$\frac{d^2y}{dt^2} + \frac{\omega_{lip}}{Q_{lip}} \frac{dy}{dt} + \omega_{lip}^2(y - y_0) = \frac{p_0 + p_u - p_d}{\mu}. \quad (2)$$

2.2 Flow equation

The lip channel is assumed to have constant width b so that the time-varying lip opening area s_{lip} is estimated by the expression $s_{lip} = 2by$. The volume-flow u through this channel is assumed to be quasi-stationary, frictionless and incompressible. Furthermore, we consider $s_{lip} \ll s_{cup}$, with s_{cup} the area of the mouthpiece entryway, and thus no pressure recovery at the mouthpiece cup. Under these assumptions, u can be expressed as a function of the pressure difference $p_0 + p_u - p_d$ across the lips using the Bernoulli equation:

$$u(t) = \sqrt{\frac{2(p_0(t) + p_u(t) - p_d(t))}{\rho}} \cdot 2by(t), \quad (3)$$

where ρ is the average air density.

3. DOWNSTREAM AND UPSTREAM FEEDBACK

3.1 Downstream coupling

According to previous studies [12–14], the downstream acoustical feedback equation can be expressed as follows:

$$p_d(t) = Z_c u(t) + \int_0^\infty r(s) \{Z_c u(t-s) + p_d(t-s)\} ds, \quad (4)$$

where $Z_c = \rho c / s_{cup}$ is the characteristic wave impedance of a cylindrical tube of cross section area s_{cup} and c is the speed of sound. $r(t)$ is the reflection function of the trombone derived from the input impedance Z_d measured experimentally using the experimental set-up described in [15].

As the reliability of the measurements becomes critical below 80 Hz, the real and imaginary parts of Z_d are linearly interpolated to zero below that value. The Fourier transform $R(\omega)$ of $r(t)$ can then be expressed as follows:

$$R(\omega) = \frac{Z_d(\omega) - Z_c}{Z_d(\omega) + Z_c}. \quad (5)$$

A quarter-period sinusoidal window is applied to $R(\omega)$ in order to remove the high frequency noise above 12 kHz. After symmetrization of $R(\omega)$ around the Nyquist frequency, $r(t)$ is calculated as the real part of the inverse Fourier transform of $R(\omega)$. The first 100 ms of $r(t)$ are represented in Fig. 2.

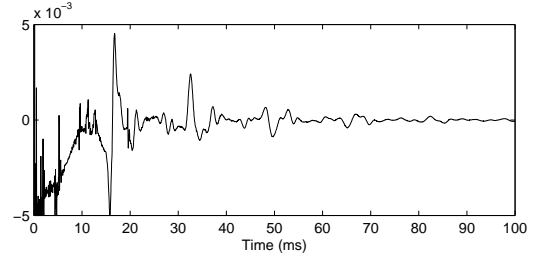


Figure 2. Reflection function $r(t)$ of a 2B King trombone (slide in the closed position) calculated from an input impedance measurement performed using the multi-microphone technique described in [15].

3.2 Upstream coupling

Contrary to previous numerical simulations of upstream coupling [16, 17], our approach does not rely on the modeling of vocal-tract resonances but only simulates an upstream feedback at f_0 . Once oscillations are established and sustained with a constant amplitude, the system is disturbed through the injection of a sinusoidal upstream acoustic pressure of the same instantaneous fundamental frequency as p_d . The amplitude of p_u is maintained constant so that the upstream acoustical feedback energy provided to the lips is constant along the tone duration. However, the instantaneous phase of p_u relative to the phase of p_d at f_0 is varied along the tone duration so that the phase difference $\angle Z_u(f_0) - \angle Z_d(f_0)$ varies linearly in time. Consequently, this protocol enables a specific investigation of the effect of the phase of the upstream impedance at f_0 , independently from the amplitude of the acoustic energy regenerated on the upstream side of the lips. This procedure is implemented according to the following looped sequence:

1. After sample $p_d(n)$ has been calculated from Eq. 4, a 2^{nd} order resonant filter (center frequency $f_c = f_{lip}$) is applied to vector $-p_d$. The output vector p_s is therefore a sinusoidal waveform of amplitude given by the resonant filter coefficients and out of phase with $p_d(f_0)$ by 180° .
2. p_s is normalized to its maximum value over its two last periods and scaled by a constant factor C . This

step enables the amplitude of acoustic upstream energy to be maintained constant, independently from the amplitude of the downstream pressure produced.

3. $p_u(n)$ is set from the normalized and scaled value of p_s , with a time-shift given by a phase-shift parameter $\Phi(n)$; $p_u(n) = p_s[n - \Phi(n)]$.
4. $p_u(n)$ is applied as in Eq. 2 and 3.
5. The procedure is iterated by one time step.

Consequently, when f_0 is constant, this procedure allows the phase difference $\angle P_u(f_0) - \angle P_d(f_0)$ to be linearly varied through the array parameter Φ . Assuming continuity of the volume flow at the reed junction [18], the following equation can be written:

$$\frac{Z_u(\omega)}{Z_d(\omega)} = -\frac{P_u(\omega)}{P_d(\omega)}, \quad (6)$$

which leads to:

$$\angle P_u(f_0) - \angle P_d(f_0) = \angle Z_u(f_0) - \angle Z_d(f_0) + \pi. \quad (7)$$

From Eq. 7, we observe that controlling the phase difference $\angle P_u(f_0) - \angle P_d(f_0)$ results in varying the phase difference $\angle Z_u(f_0) - \angle Z_d(f_0)$.

4. TIME-DOMAIN SIMULATION

Simulations are performed using the following parameter values: $f_{lip} = 310$ Hz, $Q_{lip} = 6$, $\mu = 25$ kg/m², $b = 10$ mm, $y_0 = 0$ mm, $s_{cup} = 4.8$ cm², $\rho = 1.1769$ kg/m³, $c = 347.23$ m/s. It is worth mentioning that in the downstream configuration chosen, the fifth and the sixth resonances of the downstream input impedance are respectively located around 300 Hz and 355 Hz. It is then clear that the chosen lip resonance frequency f_{lip} is between two acoustic resonances, rather than very close to one.

Time-domain simulations are performed by discretization of the differential equations using the forward Euler method and applying the trapezoidal approximation for the integration as performed in [14]. Sampling frequency is set to 48 kHz.

The quasi-static pressure p_0 is specified using a quarter-period sinusoidal onset of 10 ms, a steady phase at 15 kPa, and a quarter-period sinusoidal decay of 10 ms. The phase shift vector Φ contains values varying linearly from 110 to 240; the value contained in Φ at index n indicates the number of shifted samples applied to p_s in order to derive the p_u sample at index n . It therefore refers to the instantaneous phase shift between p_u and p_d waveforms at f_0 . The boundary values in Φ were derived empirically so that the phase shift between p_u and p_d covers the maximal range allowing the system to maintain oscillations. Scaling parameter C is set so that the p_u amplitude is of the same order of magnitude as p_d , hence producing significant effect on the system. Such order of magnitude of $P_u(f_0)/P_d(f_0)$ amplitude ratio has been observed on trombone players in the higher register [1,2]. A quarter-period sinusoidal onset

envelope is applied to the scaling factor so that the p_u amplitude grows smoothly from zero to C when injected into the system.

Simulations start with no upstream feedback ($p_u = 0$). Once the permanent regime of oscillation is reached (time t_1 determined empirically), upstream coupling is added according to the procedure described in the previous section.

5. RESULTS AND DISCUSSION

5.1 Results from simulation

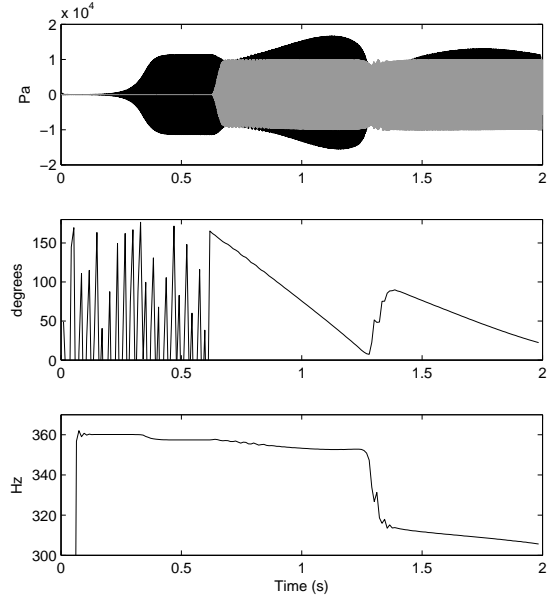


Figure 3. Results from a 96000 sample simulation at 48 kHz. From top to bottom: waveforms of p_d (black) and p_u (gray); phase difference between p_u and p_d at the fundamental frequency; fundamental frequency f_0 .

The waveforms of p_d and p_u calculated from a two-second simulation are presented in Fig. 3. Around 0.6 s, the upstream feedback is introduced and results in significant variations in p_d amplitude as the phase difference $\angle P_u - \angle P_d$ at f_0 varies linearly in time. This variation is also accompanied by changes in f_0 as shown in Fig. 3. At time 1.3 s, a change of register is observed to a lower mode, resulting in a smaller slope of the phase shift due to a smaller value of f_0 . As for the higher mode, f_0 decays slowly while $\angle P_u - \angle P_d$ is decreased until the end of the tone.

5.2 Lip mobility

The frequency response of the lip $G(\omega)$, also referred to as the lip mobility in [18], is defined as follows:

$$G(\omega) = \frac{Y(\omega)}{\Delta P(\omega)}, \quad (8)$$

where $\Delta P(\omega) = P_u(\omega) - P_d(\omega)$.

From Eq. 2, the magnitude and phase of G are represented by solid lines in Fig. 4. As predicted by the mechanical model, the outward striking character of the lip-valve system results in a $+90^\circ$ phase shift between Y and ΔP at the resonance.

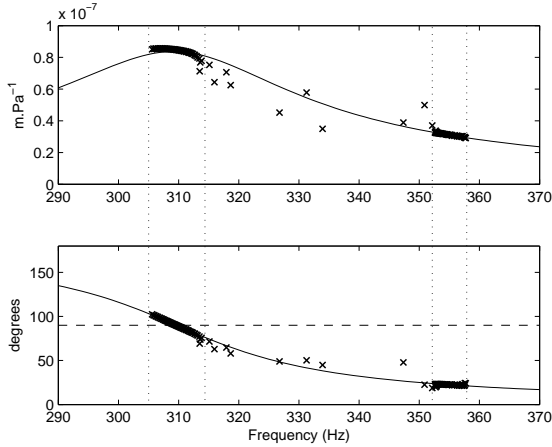


Figure 4. Amplitude (top) and phase (bottom) of lip mobility $G(\omega)$: theoretical value (solid line) and calculated from numerical simulation results (cross). The horizontal dashed line indicates 90° phase angle. The dotted lines indicate the two regions of stable oscillations corresponding to the two produced tones.

In the same figure, the amplitude and phase of the lip mobility at f_0 calculated from simulated waveforms of p_d , p_u and y are represented in crosses. As predicted by the model, and over the frequency range where acoustic energy is observed, the amplitude and phase of G estimated from simulations overlap with its theoretical values. In this particular case, variations of G at f_0 caused by the upstream feedback allow oscillations to occur over a significant frequency range, including the lip natural frequency identified by $\angle G(f_0) = 90^\circ$. This specific tuning point induces a maximum of lip displacement, hence allowing the lip valve to operate with maximal “efficiency”.

5.3 Downstream and upstream input impedances

The influence of downstream and upstream acoustical feedback can be further discussed in terms of input impedances Z_d and Z_u . The total impedance “seen” by the lip-valve $Z = -U/\Delta P$ can be expressed from Eq. 6 as the sum of the downstream and upstream impedances:

$$Z = Z_d + Z_u. \quad (9)$$

Therefore, from experimental measurement of Z_d , the complex quantities Z_u and Z can be derived from Eq. 6 and 9 at frequencies where acoustic energy is observed. The amplitude and phase of Z_d , as well as amplitude and phase of Z_u and Z over the frequency range covered, are represented in Fig. 5. For the highest tone produced with upstream support (353-358 Hz region), a decrease in Z_u amplitude is observed with decrease in frequency. This reveals a decrease in the amplitude ratio P_u/P_d at f_0 , most

probably due to the increase in $|Z_d|$. The upstream coupling also lowers the value of $\angle Z$. As $\angle Z$ becomes closer to zero, oscillations become unstable and a change of regime occurs around 353 Hz to the lower mode. Looking closer at the frequency region between 352 and 358 Hz (Fig. 6), we notice a hysteresis effect at the lower frequency limit; the change in regime occurs around 352.9 Hz when $\angle Z$ is maximized, whereas the lower playing frequency is reached around 352.7 Hz for a larger value of $\angle Z_u - \angle Z_d$ difference. In the region near the lip’s mechanical resonance (305-315 Hz interval), $|Z_u|$ roughly overlaps with $|Z_d|$, and decreasing values of $\angle Z_u$ force $\angle Z$ towards a low value plateau around -100° .

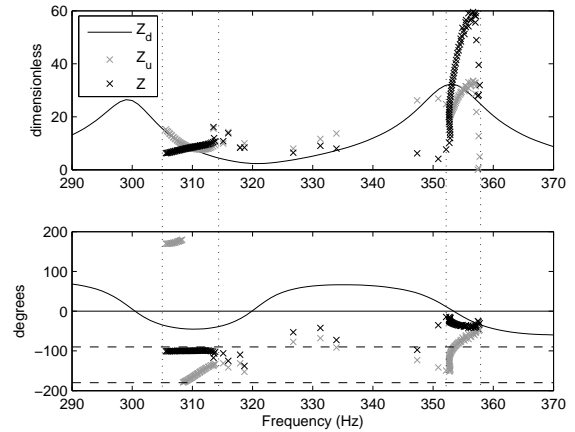


Figure 5. Amplitude (top) and phase (bottom) of $Z_d(\omega)$ measured experimentally (solid line), as well as $Z_u(\omega)$ (gray cross) and $Z(\omega)$ (black cross) at frequencies where acoustic energy is observed during simulations. The two horizontal dashed lines indicate -90° and -180° phase angles. The dotted lines indicate the two regions of stable oscillations corresponding to the two produced tones.

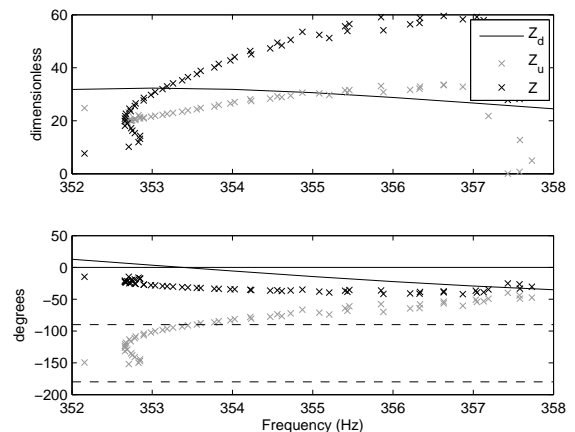


Figure 6. Closer view at Fig. 5 between 352 and 358 Hz.

These observations can be further discussed in light of the linear theory of oscillation. According to previous work [14,

18], the phase condition of regeneration under which sustained oscillations are maintained can be expressed as follows:

$$\angle Z + \angle G = 0. \quad (10)$$

This phase condition relies on the linearisation of the flow equation (Eq. 3) and therefore assumes that s_{lip} and u oscillate in phase.

From Eq. 10, we see that injection of upstream acoustic energy allowing $\angle Z$ to reach values below -90° enables $\angle G$ to extend above 90° . It thus enables oscillations to occur both above and below the lip natural frequency f_{lip} . According to Eq. 10, and given the nature of $\angle Z_d$ ($-90^\circ < \angle Z_d < 90^\circ$), oscillations could not occur at f_{lip} with an outward striking model without appropriate upstream coupling. In the 353-358 Hz region, the lowered value of $\angle Z$ enables oscillations to occur at a lower frequency and hence closer to a maximum in $|Z_d|$. In the 305-315 Hz region, the upstream coupling enables $\angle Z$ to be displaced around -100° and oscillations to occur at the lip natural frequency f_{lip} for which $\angle G = +90^\circ$.

5.4 Extension to the inward striking lip model

The lips of a brass player have been shown to potentially exhibit different mechanisms of oscillation across register [9, 11]. Overall, a transition from a dominant outward striking to dominant inward or upward striking behaviour is observed with increase in playing frequency. The theoretical evaluation presented for an outward model is extended to an inward striking model derived from Eq. 2 by setting the value of μ to -0.04 . The negative value of μ results in a negative term F_{lip} on the right side of Eq. 2. This negative force tends to close the valve when the pressure increases on the upstream side of the lips, and to open it when the pressure rises on the downstream side. The other parameters are unchanged except the equilibrium position y_0 set to 0.5 mm; by construction, this valve requires y_0 to be higher than zero in order to initiate oscillations.

The waveforms of p_d and p_u calculated from a two-second simulation are presented in Fig. 7. As in previous simulations, the upstream feedback is introduced around 0.6 s and results in significant variations in p_d amplitude as the phase difference $\angle P_u - \angle P_d$ varies linearly in time. This variation is also accompanied by changes in f_0 but without any change in register (oscillations only occur near the downstream mode located at 300 Hz). Contrary to the outward striking model, f_0 is not linearly correlated to the phase difference $\angle P_u - \angle P_d$. Injection of the disturbing signal results in a small increase in f_0 , preceding a non-linear decreasing phase until the end of the tone. Around 1.5 s, small oscillations are visible in the phase and frequency traces, as well as in the upstream pressure waveform, probably indicating a limit of stability of the system.

The values of G calculated from simulations perfectly overlap with its theoretical value as shown in Fig. 8. Contrary to the outward striking model, oscillations occur on the lower frequency side of the lip resonance. The general decrease in playing frequency induced by the phase

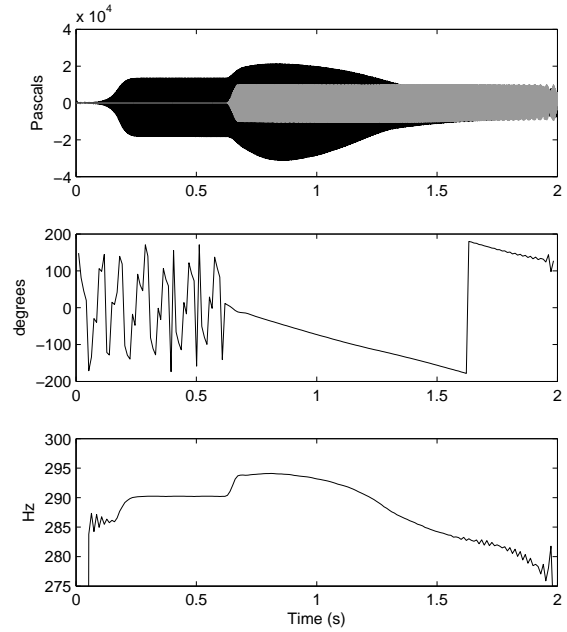


Figure 7. Results from a 96000 sample simulation at 48 kHz. From top to bottom: waveforms of p_d (black) and p_u (gray); phase difference between p_u and p_d at the fundamental frequency; fundamental frequency f_0 .

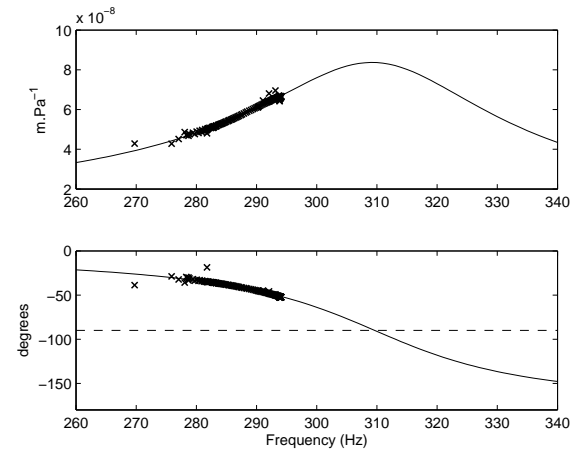


Figure 8. Amplitude (top) and phase (bottom) of lip mobility $G(\omega)$: theoretical value (solid line) and calculated from numerical simulation results (cross). The horizontal dashed line indicates -90° phase angle. The dotted lines indicate the two regions of stable oscillations corresponding to the two produced tones.

shift between P_d and P_u hence results in displacing oscillations away from the lip resonance. However, the increase in f_0 observed at the injection of the upstream perturbation tends to displace oscillations of the system closer to $|G|$ maximum. This contributes to explain the significant increase in the amplitude of p_d waveform observed in Fig. 7 between 0.65 and 0.9 s.

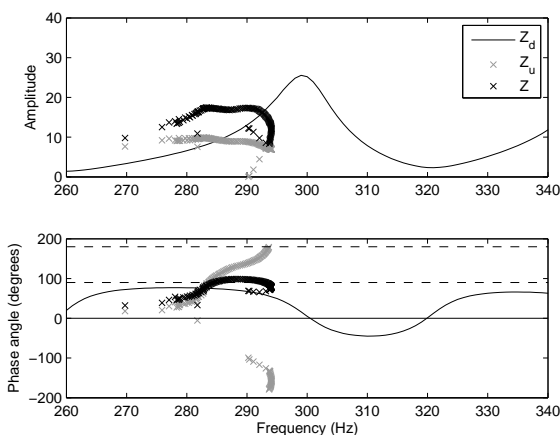


Figure 9. Amplitude (top) and phase (bottom) of $Z_d(\omega)$ measured experimentally (solid line), as well as $Z_u(\omega)$ (gray cross) and $Z(\omega)$ (black cross) at frequencies where acoustic energy is observed during simulations. The two horizontal dashed lines indicate 90° and 180° phase angles.

Looking at the amplitude and phase of Z_d , Z_u and Z at the playing frequency in Fig. 9, we observe that the upstream support allows $\angle Z$ to be raised above 90° in the region where acoustic energy is produced. According to the linear theory of oscillation, the following equality should be verified: $\angle Z = -\angle G$ as stated by Eq. 10. From Fig. 8 and 9, we observe that the validity of this relation is weak: although $\angle Z$ reaches values above 90° , $\angle G$ only decreases down to -50° . This further suggests that the downstream and upstream acoustic feedback introduce significant phase shift between the oscillatory lip opening area and acoustic flow generated at the lips.

Overall, the combined effect of the growing value of $|G|$ and $|Z_d|$ induced by the upstream coupling maximizes lip motion and lip opening area, as well as the downstream acoustic feedback. This results in boosting the amplitude of the acoustic pressure created in the mouthpiece, hence providing optimal efficiency of the sound production process.

6. CONCLUSIONS

These results focus our attention on the relevance of upstream phase tuning on the oscillation of a lip-valve system. In response to previous in-vivo and in-vitro experimental studies on the influence of upstream airways in trombone performance, this study further supports two hypothesis.

Firstly, in a region around the lips' mechanical resonance, proper upstream phase tuning may be part of trombone players' tuning strategy, so that oscillations occur very near to the mechanical resonance of the lips. Vocal-tract tuning may then result from a trade-off between the production of a high amplitude Z at f_0 , and matching f_0 with f_{lip} . However, the reasons underlying a favorable upstream phase tuning remain uncertain for the highest mode excited in

this simulation (far from the lip resonance). This should be the object of further attention.

Secondly, this method based on variations in $\angle Z_u - \angle Z_d$ at f_0 , may be implemented on an artificial player system to allow for estimation of lip natural frequency during sound production. On the contrary to other methods requiring the lips to be at rest during measurements [6, 11, 19, 20], the proposed approach enables the lip natural frequency to be evaluated while the lips are vibrating and under the constraint of the static mouth pressure. Given the sensitivity of the lips to external forces, this approach may produce more reliable estimates of f_{lip} . The results recently obtained in [4] should therefore be further analyzed with regards to identification of lip mechanical resonances.

Finally, further numerical simulations should be performed to evaluate the influence of upstream tuning on more realistic physical representations of the lips. For instance, the approach presented in this paper can be extended to the two-dimensional model proposed by Adachi [14], or two-mass models proposed by Cullen [21]. These investigations should contribute to improve our understanding of the behaviour of lip-reed valves in brass instruments, particularly with respect to the transition between different mechanisms of oscillation.

Acknowledgments

The authors would like to thank the Centre of Interdisciplinary Research in Music Media and Technology, the Schulich School of Music and the Natural Sciences and Engineering Research Council of Canada for helping fund this project.

7. REFERENCES

- [1] V. Freour and G. Scavone, "Vocal-tract influence in trombone performance," in *Proc. 2010 International Symposium on Musical Acoustics*, Sydney, Australia, 2010.
- [2] V. Fréour and G. Scavone, "Investigation of the effect of upstream airways impedance on regeneration of lip oscillations in trombone performance," in *Proc. Acoustics 2012 Nantes Conference*, Nantes, France, 2012, pp. 2225–2230.
- [3] T. Kaburagi, N. Yamada, T. Fukui, and E. Minamiya, "A methodological and preliminary study on the acoustic effect of a trumpet player's vocal tract," *J. Acoust. Soc. Am.*, vol. 130, no. 1, pp. 536–545, 2011.
- [4] V. Fréour, N. Lopes, T. Hélie, R. Caussé, and G. Scavone, "Simulating different upstream coupling conditions on an artificial trombone player system using an active sound control approach," in *Proc. ICA 2013*, Montreal, Canada, 2013.
- [5] C. Fritz, J. Wolfe, J. Kergomard, and R. Caussé, "Playing frequency shift due to the interaction between the vocal tract of the musician and the clarinet," in *Proc. Stockholm Music Acoustics Conference 2003*, 2003, p. 263266.

- [6] J. Cullen, J. Gilbert, and D. Campbell, "Brass instruments: linear stability analysis and experiments with an artificial mouth," *Acta Acustica*, vol. 86, pp. 704–724, 2000.
- [7] H. L. F. Helmholtz, *On the Sensations of Tone*. New York: Dover, 1954.
- [8] N. Fletcher, "Autonomous vibration of simple pressure-controlled valve in gas flows," *J. Acoust. Soc. Am.*, vol. 93, no. 4, pp. 2172–2180, 1993.
- [9] S. Yoshikawa, "Acoustical behavior of brass player's lips," *J. Acoust. Soc. Am.*, vol. 97, no. 3, pp. 1929–1939, 1995.
- [10] F.-C. Chen and G. Weinreich, "Nature of the lip reed," *J. Acoust. Soc. Am.*, vol. 99, no. 2, pp. 1227–1233, 1996.
- [11] J. Gilbert, S. Ponthus, and J.-F. Petiot, "Artificial buzzing lips and brass instruments: Experimental results," *J. Acoust. Soc. Am.*, vol. 104, no. 3, pp. 1627–1632, 1998.
- [12] R. Schumacher, "*Ab initio* calculations of the oscillations of a clarinet," *Acustica*, vol. 48, pp. 71–85, 1981.
- [13] S. Adachi and M. Sato, "Time-domain simulation of sound production in the brass instrument," *J. Acoust. Soc. Am.*, vol. 97, no. 6, pp. 3850–3861, 1995.
- [14] —, "Trumpet sound simulation using a two-dimensional lip vibration model," *J. Acoust. Soc. Am.*, vol. 99, no. 2, pp. 1200–1209, 1996.
- [15] A. Lefebvre and G. Scavone, "A comparison of saxophone impedances and their playing behaviour," in *Proc. 2011 Forum Acusticum*, Aalborg, Denmark, 2011.
- [16] G. Scavone, "Modeling vocal-tract influence in reed wind instruments," in *Proc. Stockholm Music Acoustics Conference 2003*, 2003, pp. 291–294.
- [17] P. Guillemain, "Some roles of the vocal tract in clarinet breath attacks: Natural sounds analysis and model-based synthesis," *J. Acoust. Soc. Am.*, vol. 121, no. 4, pp. 2396–2406, 2007.
- [18] S. Elliot and J. Bowsher, "Regeneration in brass instruments," *Journal of Sound and Vibration*, vol. 83, no. 2, pp. 181–217, 1982.
- [19] V. Fréour, R. Caussé, and K. Buys, "Mechanical behaviour of artificial lips," in *Proc. 2007 International Symposium on Musical Acoustics*, Barcelona, Spain, 2007.
- [20] M.-J. Newton, "Experimental mechanical and fluid mechanical investigations of the brass instrument lip-reed and the human vocal folds," Ph.D. dissertation, University of Edinburgh, Edinburgh, United Kingdom, 2009.
- [21] J. Cullen, "A study of brass instrument acoustics using an artificial reed mechanism, laser doppler anemometry and other techniques," Ph.D. dissertation, University of Edinburgh, Edinburgh, United Kingdom, 2000.